


Nonadiabatic transition at a band-touching point

Mohammad-Sadegh Vaezi^{1,2} and Davoud Nasr Esfahani^{2,1,*}

¹Passargad Institute for Advanced Innovative Solutions (PIAIS), Tehran 19395-5531, Iran

²Department of Converging Technologies, Khatam University, Tehran 19395-5531, Iran

 (Received 3 August 2021; revised 8 February 2022; accepted 14 February 2022; published 24 March 2022)

Low-energy Hamiltonians with a linear crossing in their energy dispersion (dubbed Dirac Hamiltonians) have recently been the subject of intense investigations. The linear dispersion is often the result of an approximation in the energy dispersion at the band-touching point in which higher order terms are discarded. In this paper, we show that, in terms of nonadiabatic transitions, by passing through a touching point, certain types of quadratic terms could not be omitted, even in the arbitrary vicinity of it, i.e., quadratic terms could significantly affect the transition probability, hence the Hamiltonian is not reducible to a linear one. We further show that the presence of terms with exponents larger than two only affects the transition probability away from the touching point. In the end, we discuss conditions that may lead to the appearance of oscillations in the transition probability profile.

DOI: [10.1103/PhysRevResearch.4.013224](https://doi.org/10.1103/PhysRevResearch.4.013224)

I. INTRODUCTION

Two-level systems (TLSs) are among the simplest quantum models due to their two-dimensional Hilbert space and manifest in a variety of physical phenomena [1–4], some of which intrinsically have only two levels (e.g., spin-half systems). Recently, they have gained considerable attention due to their applicability for simulation of quantum bits in quantum simulators and feasible applications in future quantum computation devices [5–8]. One of the well-known TLSs that has been the subject of considerable investigation is the Landau-Zener (LZ) model, which describes a gapped system such that the crossing of the simple linear energy dispersion is avoided [5,9–11]. In this model, the transition probability (TP) between the ground state and the excited state $\mathcal{P}_{LZ} = e^{-\pi\Delta^2/c}$, where Δ is the energy gap and c is the speed of the driving of the system.

Within the context of the nonadiabatic transitions, so far, most of the attention associated with TLSs has been focused on gapped systems [2,12–22]. On the other hand, there are a variety of physically relevant systems which are gapless through the presence of a touching point in the energy dispersion, e.g., graphene [23–26], 1D, and 2D p -wave superconductors [27–29], and semi-Dirac materials [30–33]. Recently, tunable construction of such gapless points has been realized in optical lattices [34–36] which are reasonable platforms for quantum simulators [37]. Noticeably, for the Dirac points, the low-energy Hamiltonian could be well approximated with TLSs by considering only the linear terms [38,39]. Nonadiabatic processes across such kinds of cones have been studied in optical lattice experiments [40–44], where away

from the touching points, any intersection of a plane parallel to the energy and y axes appears to be an avoided crossing [40]. Therefore, any transition from the ground state to the excited state could be explained based on the LZ formula in this regime (i.e., away from touching points).

For a linear crossing problem, where there is no mixing between diabatic levels (which is a gapless problem), the transition to the excited state $\mathcal{P}_{LZ} = 1$. Similarly, by nonadiabatic passage through the Dirac points, the transition to the excited state should be equal to one [40].

We know that in realistic physical systems a perfect linear crossing does not exist. That is, linear models are low-energy Hamiltonians where higher order terms are neglected at the proximity of coalescence points. In this paper, we show that in the context of nonadiabatic transitions, such Hamiltonians are not reducible to a linear one (i.e., no matter how close we are to the touching point in the parameter space). To this end, we employ the concept of fidelity susceptibility (FIS), hereafter denoted by χ [45]. We consider a Hamiltonian $\hat{H}(\lambda)$ with a touching point at $\lambda = 0$. By expanding $\hat{H}(\lambda)$ around $\lambda = 0$, we prove that if certain quadratic terms are neglected, $\chi(\lambda) \rightarrow 0$ as $\lambda \rightarrow 0$, while keeping them, results in a finite $\chi(\lambda)$ as $\lambda \rightarrow 0$. We then show that such nonvanishing $\chi(0)$ leads to a TP less than one upon nonadiabatic passage through the touching point. Furthermore, we discuss the TP far away from the touching point based on FIS.

The outline of this paper is as follows. In Sec. II, we briefly review the concept of FIS and its relation with the TP. In Sec. III, we investigate FIS for two interesting gapless models followed by relevant discussions. Qualitative analysis and numerical results are provided in Secs. IV and V, respectively. We summarize our main message and findings in Sec. VI.

II. FIDELITY SUSCEPTIBILITY AND NONADIABATIC TRANSITIONS

Let us consider a TLS which is explained based on a Hamiltonian $\hat{H}(\lambda)$, where λ is a real scalar. A convenient

*d.nasr@khatam.ac.ir; dd.nasr@gmail.com

Published by the American Physical Society under the terms of the [Creative Commons Attribution 4.0 International license](https://creativecommons.org/licenses/by/4.0/). Further distribution of this work must maintain attribution to the author(s) and the published article's title, journal citation, and DOI.

way for investigation of the time evolution of such systems, with a discrete basis set, is to represent the evolved wave function based on the instantaneous basis set, i.e., $|\psi(t)\rangle = \sum_{n=0,1} c_n(t)|n(\lambda(t))\rangle$, where $|n(\lambda(t))\rangle$ s are the eigenstates of the following time-independent Schrodinger equation $H(\lambda(t))|n_\lambda(t)\rangle = E_n(t)|n_\lambda(t)\rangle$, and t denotes time. In this representation, the equation of motion for each $c_n(t)$ reads [46]

$$\dot{c}_n(t) = - \sum_{m \neq n} e^{i\theta_{nm}(t)} \tilde{c}_m(t) \dot{\lambda} \frac{\langle n_\lambda(t) | \partial_\lambda H(\lambda(t)) | m_\lambda(t) \rangle}{(E_m - E_n)}, \quad (1)$$

where $\theta_{nm}(t) = \theta_n(t) - \theta_m(t)$, $\theta_n(t) = \int_0^t E_n(\tau) d\tau - i \int_0^t \langle n_\lambda(\tau) | \dot{n}_\lambda(\tau) \rangle d\tau$, and $\tilde{c}_n(t) = c_n(t) e^{i\theta_n(t)}$. Therefore, starting from one of the eigenstates of the Hamiltonian, if the system is driven by changing λ with a pace of $\dot{\lambda}$, one may expect that larger $\dot{\lambda} \frac{\langle n_\lambda(t) | \partial_\lambda H(\lambda(t)) | m_\lambda(t) \rangle}{(E_m - E_n)}$ would acquire larger transition to the other state.

For TLSs, the absolute value of $\frac{\langle n_\lambda(t) | \partial_\lambda H(\lambda(t)) | m_\lambda(t) \rangle}{(E_m - E_n)}$ with $n \neq m$ is nothing but the square root of FIS associated with the n th level, i.e., $\chi_n(\lambda)$. Here $\chi_0(\lambda) = \chi_1(\lambda) = \chi(\lambda)$ holds.

It is known that FIS can be employed as a general measure of phase transitions [45,47]. Moreover, FIS has been utilized as a qualitative upper bound for TP [48] and is instrumental for the comparison of ground-state probability of driven systems with different ground-state orders [49].

When there is a gap in the system, semiclassical analysis is a well-established method for the estimation of a TP. In particular, the Dykhne-Davis-Pechukas (DDP) [50,51] method widely has been employed for the estimation of nonadiabatic TPs of TLSs [17,18,20]. While DDP seems to be very successful, it has two drawbacks. First, it works only for gapped models, i.e., the instantaneous eigenstates of the model must not cross in real time [17,18,20,50,51] (yet they may cross in complex time domain). Second, it gives an estimate of TP for a driving $t = -\infty \rightarrow +\infty$. Hence, one may lose information about intermediate transitions throughout the evolution. Fortunately, by employing often low-cost numerical integration of time-dependent Schrodinger equation for TLSs, one may achieve rather accurate results for the magnitude of TPs for both gapped and gapless models.

Based on the above-mentioned discussions, since we mainly focus on gapless models, in the rest of this paper we will use FIS to detect active regions of the phase space where a transition to the other state is more likely. We should note that due to the role of θ_{mn} (which is related to the band structure and geometrical phase [46]) in Eq. (1), if two systems have the same FIS, we cannot necessarily assert that they have the same nonadiabatic behavior.

Throughout the rest of this paper, we will suppose that all of the systems are driven such that $\lambda(t) = ct$. To numerically evolve $|\psi(t)\rangle$ in time, we will employ the Crank-Nikelson method [52]. For all numerical simulations we consider $\hbar = 1$ and set the time step equal to 0.001.

By starting from some $|\phi_0(\lambda(t_i))\rangle$, we define the TP $\mathcal{P} = |\langle \phi_1(\lambda(t_f)) | \psi(t_f) \rangle|^2$ at specific final t_f . The $\lambda(t_i)$ and $\lambda(t_f)$ are fixed by the protocol of driving. The 0 and 1 subscripts denote the instantaneous ground state and excited state respectively.

We further define the following protocols of driving of the Hamiltonians under study: PL₁ corresponds to a driving

$-\lambda_0 \rightarrow \lambda_0$, where λ_0 is a starting point which is very close to touching point. Here we fix $\lambda_0 = 0.1$. PL_{−∞,0} corresponds to a driving $\lambda(-\infty) \rightarrow \lambda(0)$ and PL_{0,∞} corresponds to a driving from $\lambda(0) \rightarrow \lambda(+\infty)$. PL₂ is assigned for a driving $\lambda(-\infty) \rightarrow \lambda(+\infty)$.

III. MODELS AND DISCUSSIONS

We start with a gapless Hamiltonian corresponding to the boundary of a trivial and topological phase of a p -wave superconductor [29],

$$H_{\text{PW}}(\lambda) = \begin{pmatrix} \frac{\lambda^2}{2m} & \lambda\Delta \\ \lambda\Delta^* & -\frac{\lambda^2}{2m} \end{pmatrix},$$

where λ is momentum, m mass of electron, and $\lambda\Delta$ is the linear coupling. The energy dispersion $E(\lambda) = \pm |\lambda| \sqrt{\frac{\lambda^2}{4m^2} + |\Delta|^2}$, with a touching point at $\lambda = 0$. The corresponding FIS reads

$$\chi(\lambda) = \left(\frac{2m\Delta}{(2m\Delta)^2 + \lambda^2} \right)^2, \quad (2)$$

with the property $\lim_{\lambda \rightarrow 0} \chi(\lambda) = 1/4m^2\Delta^2$. For finite values of m , one may be tempted to ignore the diagonal terms in the Hamiltonian for small enough values of λ near 0, which results in an approximated Hamiltonian $\tilde{H}_{\text{PW}}(\lambda) = \begin{pmatrix} 0 & \lambda\Delta \\ \lambda\Delta^* & 0 \end{pmatrix}$ with $\tilde{\chi}(\lambda) = 0$. Here the two diabatic bands become completely unperturbed. However, this is in stark difference with what we found earlier for FIS, i.e., $\lambda \rightarrow 0$, $\chi(\lambda) \rightarrow 1/4m^2\Delta^2$. Based on our discussions in Sec. II, this shows that, in terms of time evolution of the system, H_{PW} is not reducible to a simple linear model even for very small values of λ . It is worth mentioning that only when $m \rightarrow \infty$, ignoring the quadratic terms is a valid approximation.

As an another instructive example, we consider the low-energy Hamiltonian for a graphenelike system with a prominent property that acquires a gapless point at $\mathbf{K} = \frac{2\pi}{3a}(1, \frac{1}{\sqrt{3}})$. The tight-binding Hamiltonian is given by [39]

$$H_{\text{GR}} = \begin{pmatrix} 0 & s(\mathbf{k}) \\ s^*(\mathbf{k}) & 0 \end{pmatrix}, \quad (3)$$

where $s(\mathbf{k}) = -he^{-ik_x a} (1 + 2e^{i(\frac{3k_y a}{2})} \cos \frac{\sqrt{3}}{2} k_y a)$, h is the hopping parameter, and a is the lattice constant. Often, the full Hamiltonian is approximated with a low energy one that is linear around \mathbf{K} . Here, we show that as long as nonadiabaticity is under consideration, quadratic terms could become important corresponding to a passage through the coalescence point. To this end, we expand $s(\mathbf{k})$ around \mathbf{K} up to second order (i.e., $\mathbf{k} \rightarrow \mathbf{K} + \mathbf{q}$). Therefore,

$$H = -\frac{3ha}{2} \begin{pmatrix} 0 & \alpha(q_y - iq_x) \\ \alpha^*(q_y + iq_x) & 0 \end{pmatrix} - \frac{3ha^2}{8} \begin{pmatrix} 0 & \alpha(q_y + iq_x)^2 \\ \alpha^*(q_y - iq_x)^2 & 0 \end{pmatrix}, \quad (4)$$

where $\alpha = e^{i\frac{2\pi}{3}}$. Since we are interested in studying TPs for passages through the Dirac points, we set $q_y = 0$, $q_x = \lambda$. By eliminating α through an appropriate gauge transformation,

the Hamiltonian reads

$$H(\lambda) = \gamma \begin{pmatrix} 0 & 2i\lambda + a\lambda^2/2 \\ -2i\lambda + a\lambda^2/2 & 0 \end{pmatrix}. \quad (5)$$

The corresponding energy dispersion $E_{\pm} = \pm\gamma|\lambda|\sqrt{(a\lambda/2)^2 + 4}$, where $\gamma = 3ah/4$ and the touching point occurs at $\lambda = 0$. The above-mentioned Hamiltonian could be transformed to a PW-type Hamiltonian through the global gauge transformation $U = \frac{1}{\sqrt{2}} \begin{pmatrix} e^{i\pi/4} & e^{-i\pi/4} \\ e^{i\pi/4} & -e^{-i\pi/4} \end{pmatrix}$. The transformed Hamiltonian ($U^\dagger H U$) is

$$H(\lambda) = -\gamma \begin{pmatrix} -\frac{a\lambda^2}{2} & 2\lambda \\ 2\lambda & \frac{a\lambda^2}{2} \end{pmatrix}, \quad (6)$$

with

$$\chi(\lambda) = \left(\frac{4a}{a^2\lambda^2 + 16} \right)^2. \quad (7)$$

Obviously, similar to χ_{PW} , χ does not become zero at the touching point. Noticeably, $\chi(0)$ is only a function of lattice constant a , thus could be tuned by the strain. We should note that the presence of the phase difference between the linear and quadratic term is essential for χ to become nonzero at $\lambda = 0$.

If we keep only the linear term in Eq. (5), trivially χ becomes zero. This means that a transition to the excited state occurs with a probability equal to one. However, Eq. (7) tells us that the TP to the excited state becomes less than one, as $\chi(0) \neq 0$ (even in the arbitrary vicinity of the touching point).

It is worth mentioning that when $q_y \neq 0$, by only considering the linear terms for q_x , the problem will be reduced to a basic LZ problem, where LZ formula gives a fairly good estimation of the tunneling probability [40].

To figure out the effect of larger order terms in the above-mentioned examples, we consider the following Hamiltonian:

$$H = \begin{pmatrix} g(\lambda) & \Delta\lambda \\ \Delta\lambda & -g(\lambda) \end{pmatrix}, \quad (8)$$

where $g(\lambda) = \sum_{n=1..N} a_n \lambda^n$ and λ and Δ are real numbers. The corresponding $\chi(\lambda)$ has the following form:

$$\chi(\lambda) = \left(\frac{\Delta}{2} \times \frac{a_2 + \lambda k(\lambda)}{\Delta^2 + (g(\lambda)/\lambda)^2} \right)^2, \quad (9)$$

with $k(\lambda) = \sum_{n=2..N-1} n a_{n+1} \lambda^{n-2}$. One can easily check that as $\lambda \rightarrow 0$, then $\chi(\lambda) \propto a_2^2$, which is nonzero as long as $a_2 \neq 0$. This means that $\chi(0)$ is only affected by second-order terms. The terms with an exponent larger than two will affect χ only away from the touching.

To better understand the role of terms with exponents larger than two in Eq. (8), one may define

$$H_{\text{GL}}^{(n)}(\lambda) = \begin{pmatrix} \lambda^n & \lambda\Delta_1 \\ \lambda\Delta_1 & -\lambda^n \end{pmatrix}, \quad (10)$$

with

$$\chi_{\text{GL}}^{(n)}(\lambda) = \frac{(n-1)^2 \Delta_1^2 \lambda^{2(n-2)}}{4(\Delta_1^2 + \lambda^{2(n-1)})^2}. \quad (11)$$

In the following section, we will first qualitatively analyze $\mathcal{P}_{\text{GL}}^{(n)}$ for $n = 1, 2$ where $n = 2$ corresponds to H_{PW} . For $\mathcal{P}_{\text{GL}}^{(n>2)}$,

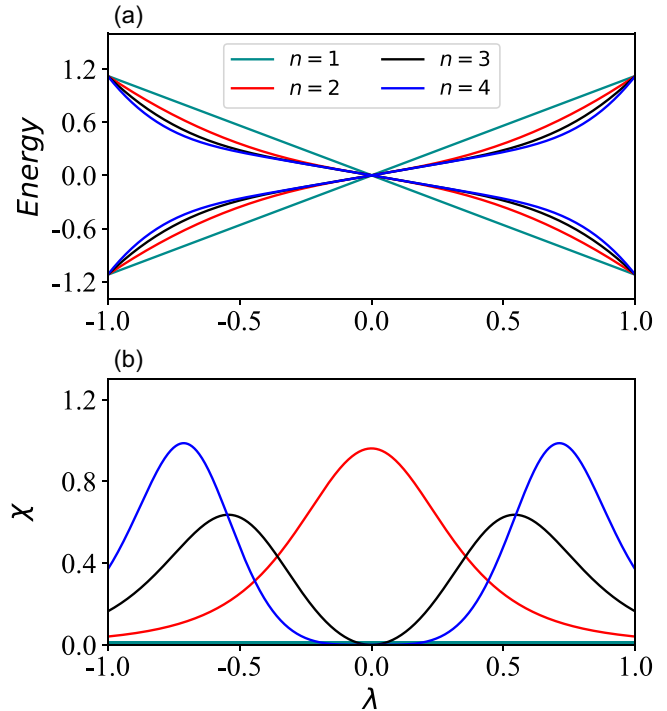


FIG. 1. (a) Energy dispersion as a function of parameter λ . (b) The FIS as a function of λ for different orders of diagonal part of gapless Hamiltonian, $H_{\text{GL}}^{(n)}$ and for $\Delta_1 = 0.5$.

we observe, in general, two distinct behaviors for even and odd values of n . Hereafter, we refer to Δ_1 as the linear coupling.

IV. QUALITATIVE ANALYSES

In this section, we qualitatively analyze the behavior of TPs for each $H_{\text{GL}}^{(n)}(\lambda)$ for different values of n . As we will see in our models, the dispersion of $\chi(\lambda)$ consists of different peaks. Therefore, for the sake of simplicity, we label the location of the peaks with MFP (maximum fidelity point). For the location of the minimum gap, we use MGP (minimum gap point).

$H_{\text{GL}}^{(1)}(\lambda)$: This model is gapless with $\lambda_{\text{MGP}} = 0$, and $\chi(\lambda) = 0$ everywhere. Therefore, by passing through the crossing point, the transition to the excited state becomes one for both adiabatic and nonadiabatic regimes, with no change in the character of the initial state.

$H_{\text{GL}}^{(2)}(\lambda)$ (1D p -wave like Hamiltonian): Here, $\lambda_{\text{MGP}} = \lambda_{\text{MFP}} = 0$ (see Fig 1) and $\chi(\lambda) = \frac{\Delta_1^2}{4(\lambda^2 + \Delta_1^2)^2}$ [which is similar to $\chi(\lambda)$ of the LZ]. Since $\chi(0) \neq 0$, therefore different from $H_{\text{GL}}^{(1)}$, the nonadiabatic transition is not equal to one for a finite speed of the driving of the system through the touching point. Here, the faster one drives the system, the probability that the evolved state remains in the instantaneous ground state becomes larger, and there is no change of the character for fast enough speeds (for numerical results see Sec. V).

For an adiabatic evolution, the evolved state acquires a change of the character by passing through the crossing point, and a transition to the excited state occurs with a TP equal to one. As explained in Sec. III, $H_{\text{GL}}^{(2)}$ is not reducible to a

linear Hamiltonian in terms of both adiabatic and nonadiabatic evolution.

$H_{\text{GL}}^{(n=\text{odd})}(\lambda)$: In this case, χ acquires a two peak structure as a function of λ with $\lambda_{\text{MGP}} = 0$ and $\lambda_{\pm, \text{MFP}} = \pm (\frac{n-2}{n} \Delta_1^2)^{\frac{1}{2(n-1)}}$ (see Fig. 1). Different from $H_{\text{GL}}^{(2)}$, $\chi(\lambda)$ acquires its minimum at λ_{MGP} , i.e., $\chi(\lambda_{\text{MGP}}) = 0$. That is, upon passing through the touching point with a PL_1 protocol, the transition to the excited state almost happens without a change of the character of the evolved wave function. In other words, as long as the starting state of the evolution process is the ground state of the system which is close enough to the touching point, the system is reducible to a simple crossing Hamiltonian in terms of nonadiabatic transition (i.e., ignoring the diagonal cubic terms in the Hamiltonian might be a good approximation).

For a PL_2 protocol, apart from the physical relevance of such a model, because $H_{\text{GL}}^{(n=\text{odd})}(-\lambda) = -H_{\text{GL}}^{(n=\text{odd})}(\lambda)$, the wave function propagates back in time by passing through the touching point. Therefore, a transition to the excited state with a probability equal to one is warranted (without a change of character).

$H_{\text{GL}}^{(n=\text{even})}(\lambda)$: This situation is very similar to what was discussed about $H_{\text{GL}}^{(n=\text{odd})}$. That is, $H_{\text{GL}}^{(n=\text{even})}$ is reducible to a simple crossing model close enough to the touching point. However, different from $H_{\text{GL}}^{(n=\text{odd})}$, the $H_{\text{GL}}^{(n=\text{even})}(-\lambda) \neq -H_{\text{GL}}^{(n=\text{even})}(\lambda)$. Therefore, the evolution of the system is not as trivial as odd cases.

If the starting point of the evolution process is considered far away from the touching point, i.e., beyond one of the MFP points, then upon nonadiabatic driving of the system through the MGP (a PL_2 protocol), the TP can be understood at two asymptotic limits of large and small values of Δ_1 .

When $\Delta_1 \ll 1$, we have $c\sqrt{\chi} \gg 1$. Then, the system is highly nonadiabatic and the evolved wave function preserves its initial form, which results in $\mathcal{P} \ll 1$.

On the other hand, $c\sqrt{\chi} \ll 1$ when $\Delta_1 \gg 1$ (adiabatic limit). In this limit, the evolved wave function will have a large contribution from the ground state (the excited state) for $\lambda(t) < 0$ ($\lambda(t) > 0$). Consequently, $\mathcal{P} \sim 1$, and a change of character from $|\psi(-\infty)\rangle = \binom{0}{1}$ to $|\psi(+\infty)\rangle = \binom{1}{0}$ occurs.

For the intermediate values of Δ_1 , \mathcal{P} interpolates between these two limits.

V. NUMERICAL RESULTS

To complement the analyses in the previous section, here we provide our numerical findings for TP. As explained in Sec. IV, $H_{\text{GL}}^{(n=\text{odd})}$ has a trivial time evolution behavior. Hence, we ignore it in the remainder of our discussion.

Since, in the context of nonadiabatic transitions, gapped systems have been well studied in the past, it would be good practice to compare our results for gapless models with those of gapped systems with the same order of diagonal terms. To this end, we define [18–20]

$$H_{\text{GP}}^{(n)}(\lambda) = \begin{pmatrix} \lambda^n & \Delta_2 \\ \Delta_2 & -\lambda^n \end{pmatrix}, \quad (12)$$

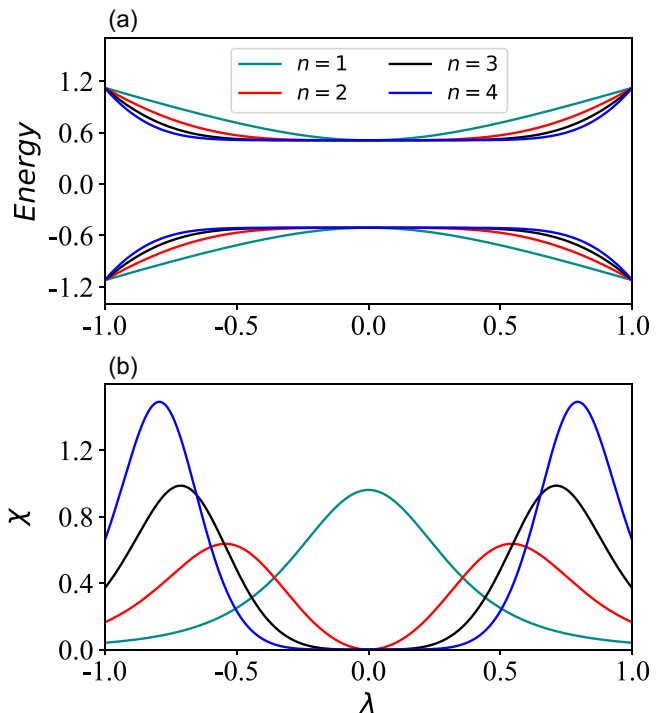


FIG. 2. (a) Energy dispersion as a function of parameter λ . (b) The FIS as a function of λ for different orders of diagonal part of gapped Hamiltonian, $H_{\text{GP}}^{(n)}$ and for $\Delta_2 = 0.5$.

for which

$$\chi_{\text{GP}}^{(n)}(\lambda) = \frac{n^2 \Delta_2^2 \lambda^{2(n-1)}}{4(\Delta_2^2 + \lambda^{2n})^2}, \quad (13)$$

with $\lambda_{\text{MGP}} = 0$ and $\lambda_{\pm, \text{MFP}} = \pm (\frac{n-1}{n+1} \Delta_1^2)^{\frac{1}{2n}}$ (see Fig. 2). Setting $n = 1$, $H_{\text{GP}}^{(1)}$ is nothing but a basic LZ Hamiltonian. One can also check that $\chi_{\text{GP}}^{(n-1)} \equiv \chi_{\text{GL}}^{(n)}$.

Similar to the Hamiltonian of each model, the TP is labeled with the GL/GP and order n . The details of the method employed for the time evolution, the definition of TP (\mathcal{P}), and the definition of driving protocols are explained in Sec. II.

In Fig. 3(a), $\mathcal{P}_{\text{GL}}^{(n)}$ is plotted as a function of Δ_1 , with a PL_2 protocol and for different values of $n = 2, 4, 6, 8$. For all cases, by increasing Δ_1 , $\mathcal{P}_{\text{GL}}^{(n)}$ monotonously is enhanced, which is in accord with our qualitative analyses in Sec. IV. That is, by increasing Δ_1 , FIS is suppressed. Consequently, the system approaches the adiabatic regime which results in a TP equal to one.

In Fig. 3(b), we have the same plot as Fig. 3(a) but for a PL_1 protocol. Obviously, $\mathcal{P}_{\text{GL}}^{(n)} \simeq 1$ for $n > 2$ cases, which means nonlinear diagonal terms (λ^n) have a very marginal effect on the TP as long as the starting point is close enough to the touching point, which is the case for a PL_1 protocol. This is also in agreement with our qualitative analysis. That is, near the crossing point, the FIS becomes very small and a complete TP to the excited state is expected. However, $\mathcal{P}_{\text{GL}}^{(2)}$ shows a different behavior for a PL_1 protocol in comparison with $n > 2$ cases. In this case, when $\Delta_1 \rightarrow 0$, $\mathcal{P}_{\text{GL}}^{(2)} \rightarrow 0$. The reason for such behavior is that when $\lambda \rightarrow 0$, then $\chi \rightarrow \frac{1}{\Delta_1}$. Consequently, χ is enhanced when $\Delta_1 \rightarrow 0$. This means the

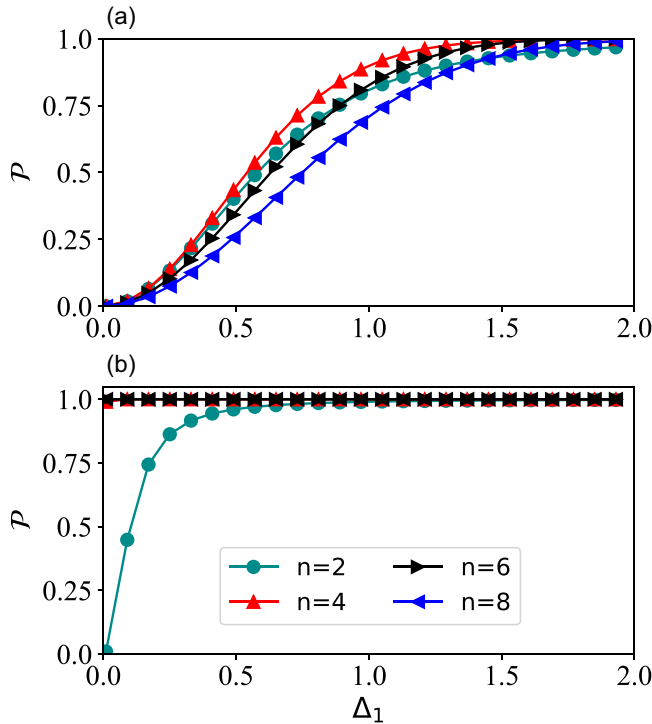


FIG. 3. The $\mathcal{P}_{\text{GL}}^{(n)}$ as a function of the linear coupling Δ_1 , with $n = 2, 4, 6, 8$ and $c = 0.1$ for PL₂ (a) and PL₁ (b) protocols.

system is still highly nonadiabatic for small values of Δ_1 which finally results in a suppressed transition to excited state for small values of Δ_1 .

In Fig. 4(a), $\mathcal{P}_{\text{GP}}^{(1)}$ ($\equiv \mathcal{P}_{\text{LZ}}$) is plotted versus Δ_2^2 and for different values of c . As expected, it decays exponentially as a function of Δ_2^2 and decreases as c becomes smaller.

Figure 4(b) shows $\mathcal{P}_{\text{GL}}^{(2)}$ versus Δ_1^2 and for different values of c . The figure depicts that $\mathcal{P}_{\text{GL}}^{(2)}$ is increased simultaneous to the enhancement of Δ_1^2 , and is suppressed upon the amplification of c , which is in stark difference with $\mathcal{P}_{\text{GP}}^{(1)}$. Interestingly, $\mathcal{P}_{\text{GL}}^{(2)}$ reveals that the evolved wave function tends to have larger ground-state contribution by increasing the speed of driving.

As discussed before, the TP for gapless models shows a monotonous enhancement toward one as a function of the linear coupling.

Now we compare the TP of gapped and gapless models with the same order n . In Fig. 5(a), $\mathcal{P}_{\text{GP}}^{(4)}$ is plotted as a function of Δ_2 , as expected from semiclassical analysis of the TP [17,20], an oscillating behavior as a function of Δ_2 is observed. Based on the DPP method, such oscillation arises from the zeros of the energy difference between the two states. Such zeros consist of both real and imaginary parts, which finally result in an oscillatory behavior in $\mathcal{P}_{\text{GP}}^{(4)}$ [17]. The oscillatory behavior prevails for $\mathcal{P}_{\text{GP}}^{(n)}$ with arbitrary $n > 1$.

In Fig. 5(b), we also depict $\mathcal{P}_{\text{GL}}^{(4)}$ as a function of the linear coupling and for different speeds of driving, which shows a monotonous enhancement of $\mathcal{P}_{\text{GL}}^{(4)}$ to one as a function of Δ_1 and $1/c$.

Oscillations of $\mathcal{P}_{\text{GP}}^{(4)}$ as a function of Δ_2 could be explained based on a real-time analysis through a gap-dependent

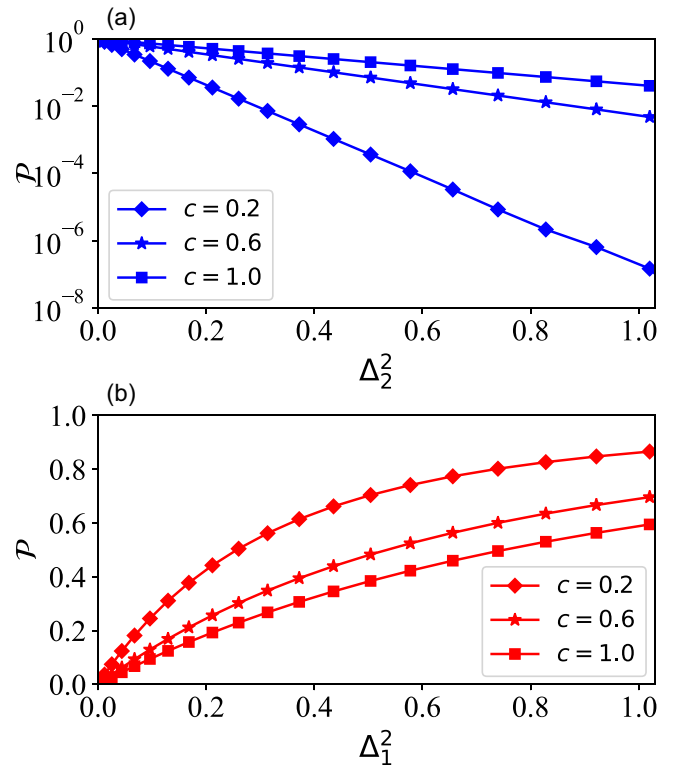


FIG. 4. (a) $\mathcal{P}_{\text{GP}}^{(1)}$ as a function of Δ_2^2 in log scale and for different speeds of driving c . (b) $\mathcal{P}_{\text{GL}}^{(2)}$ as a function of Δ_1^2 for different speeds of driving c . Solid lines are guides for eye.

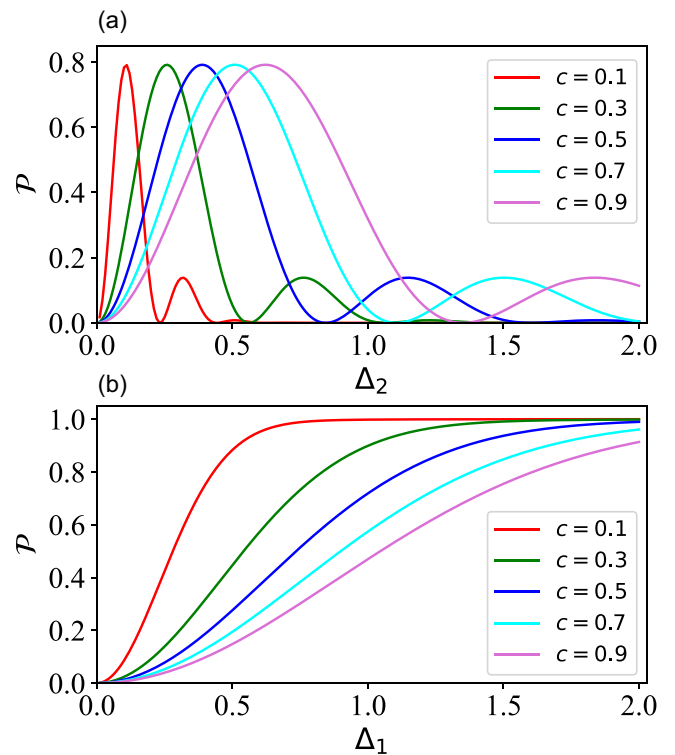


FIG. 5. (a) Transition probability, $\mathcal{P}_{\text{GP}}^{(4)}$, as a function of Δ_2 and different speeds of driving c for a PL₂ protocol. (b) $\mathcal{P}_{\text{GL}}^{(4)}$, as a function of Δ_1 and different speeds of driving c for a PL₂ protocol.

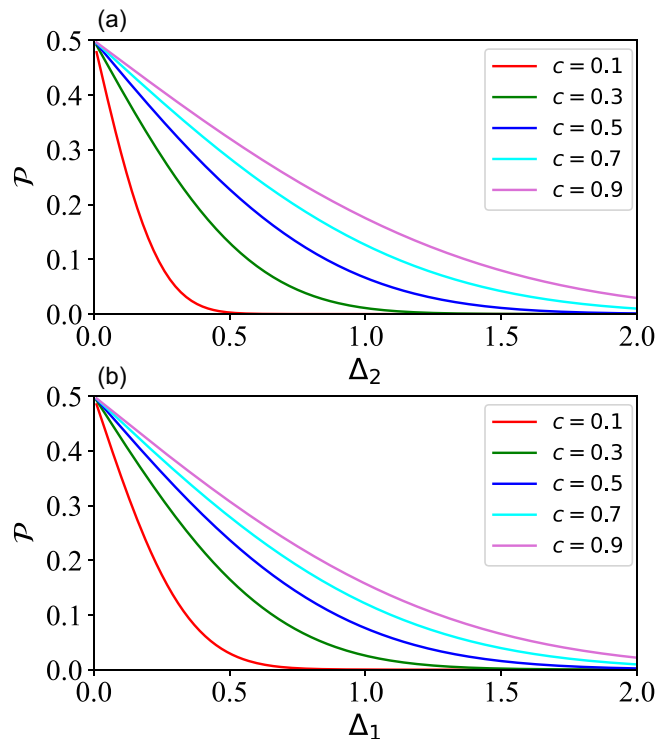


FIG. 6. (a) $\mathcal{P}_{\text{GP}}^{(4)}$ as a function of Δ_2 , for a $\text{PL}_{-\infty,0}$ protocol with different speeds of driving c . (b) $\mathcal{P}_{\text{GL}}^{(4)}$ as a function of the linear coupling Δ_1 for $\text{PL}_{-\infty,0}$ protocol with different speeds of driving c .

interference of the two peaks in the dispersion of χ for a PL_2 protocol, where a passage through both peaks occurs. Moreover, monotonous $\mathcal{P}_{\text{GL}}^{(4)}$ as a function of Δ_1 behavior is a signature of a fixed interference between the two peaks, which does not depend on Δ_1 . This is generally correct for $\mathcal{P}_{\text{GL}}^{(n)}$ with even $n > 2$.

To elaborate on the interference of the two peaks in gapped (for $n > 1$) and gapless models (for $n > 2$), since there are two major peaks at $\lambda_{\pm, \text{MFP}}$ separated by a region with $\chi \simeq 0$ in the spectrum of χ (as a function of λ), we divide PL_2 into a $\text{PL}_{-\infty,0}$ followed by a $\text{PL}_{0,\infty}$. We first compare $\mathcal{P}_{\text{GP}}^{(4)}$ and $\mathcal{P}_{\text{GL}}^{(4)}$ for a $\text{PL}_{-\infty,0}$ protocol, which consists of passing through $\lambda_{-\text{MFP}}$. In practice, for the case of gapless models, we evolve from $-\infty$ to $-\epsilon$, where ϵ is an infinitesimal positive number. In Fig. 6(a), for a $\text{PL}_{-\infty,0}$ driving, the $\mathcal{P}_{\text{GP}}^{(4)}$ is depicted as a function of Δ_2 and for different speeds of driving. A clear observation is that the TP monotonously fades as a function of Δ_2 . The same is observed for $\mathcal{P}_{\text{GL}}^{(4)}$ subjected to a $\text{PL}_{-\infty,0}$ driving as a function of the linear coupling Δ_1 . The latter is depicted in Fig. 6(b). Clearly, \mathcal{P} behaves very similarly for both GP and GL cases and there is no oscillation in $\mathcal{P}_{\text{GP}}^{(4)}$ and $\mathcal{P}_{\text{GL}}^{(4)}$ as a function of Δ_2 and Δ_1 , respectively.

Next we look at the effect of $\text{PL}_{0,\infty}$ on the result of $\text{PL}_{-\infty,0}$. This could be explained as follows. Starting from the instantaneous ground state at $t = -\infty$, we evolve the wave function from $t = -\infty$ to $t = 0$, where $\chi \simeq 0$ in this region. Then, by writing the evolved wave function based on instantaneous eigenstates at $t = 0$, we evolve each of the instantaneous eigenstates to $t = +\infty$; the final evolved state at $t = +\infty$ is the superposition of the evolved instantaneous eigenstates at

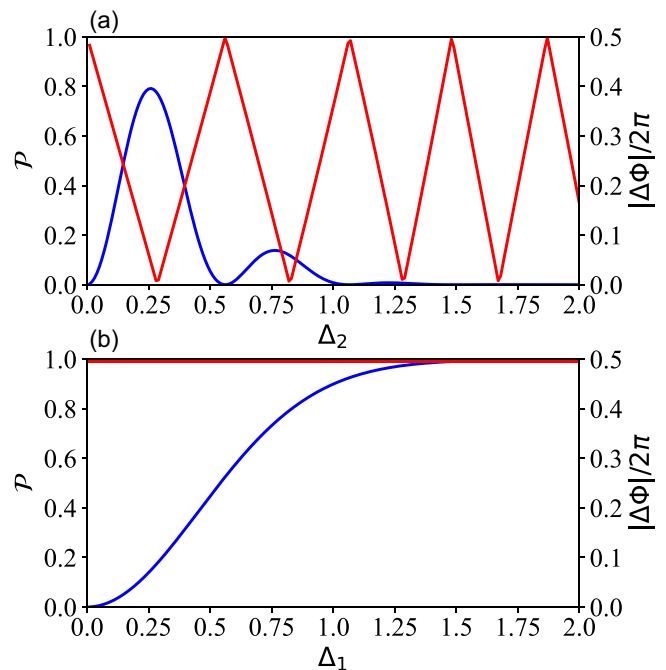


FIG. 7. (a) $\mathcal{P}_{\text{GP}}^{(4)}$ (blue) and $|\Delta\Phi|/2\pi$ (red) as a function of coupling Δ_2 for a PL_2 protocol with $c = 0.3$. (b) $\mathcal{P}_{\text{GL}}^{(4)}$ (blue) and $|\Delta\Phi|/2\pi$ (red) as a function of the linear coupling Δ_1 for a PL_2 protocol with $c = 0.3$.

$t = 0$. The result of the TP must be exactly the same as the single PL_2 protocol. This could be written as follows:

$$\begin{aligned} |\psi(t = +\infty)\rangle &= U(+\infty, 0)U(0, -\infty)|\phi_0(t = -\infty)\rangle \\ &= U(+\infty, 0)(\alpha_+|\phi_1(0)\rangle + \alpha_-|\phi_0(0)\rangle) \\ &= (\alpha_+\beta_+^+ + \alpha_-\beta_-^+)|\phi_1(+\infty)\rangle \\ &\quad + (\alpha_+\beta_+^- + \alpha_-\beta_-^-)|\phi_0(+\infty)\rangle, \end{aligned} \quad (14)$$

where $\alpha_{\pm} = \langle\phi_{1,0}(0)|U(0, -\infty)|\phi_0(-\infty)\rangle$, $\beta_{\pm}^{\pm} = \langle\phi_{1,0}(+\infty)|U(+\infty, 0)|\phi_1(0)\rangle$ and $\beta_{\pm}^{\mp} = \langle\phi_{1,0}(+\infty)|U(+\infty, 0)|\phi_0(0)\rangle$. Therefore TP $\mathcal{P} = |\alpha_+\beta_+^+ + \alpha_-\beta_-^+|^2$. By writing $\alpha_{\pm} = |\alpha_{\pm}|e^{ia_{\pm}}$, $\beta_{\pm}^+ = |\beta_{\pm}^+|e^{ib_{\pm}^+}$, and $\beta_{\pm}^- = |\beta_{\pm}^-|e^{ib_{\pm}^-}$, the TP could be written as

$$\mathcal{P}_{\text{tr}} = |\alpha_+\beta_+^+|^2 + |\alpha_-\beta_-^+|^2, \quad (15)$$

$$+ 2|\alpha_+\beta_+^+| \times |\alpha_-\beta_-^+| \cos\Delta\Phi, \quad (16)$$

where $\Delta\Phi = \text{Im} \ln[\alpha_+\beta_+^+(\alpha_-\beta_-^+)^*] = [a_+ + b_+ - a_- - b_-]_{\text{mod } 2\pi}$, with $\Xi_{\text{mod } 2\pi} = \Xi \text{ mod } 2\pi - \pi$. $\Delta\Phi$ is the indicator of the interference of the two peaks in the spectrum of χ .

In Fig. 7(a), $\mathcal{P}_{\text{GP}}^{(4)}$ is plotted for a $\text{PL}_2 = \text{PL}_{-\infty,0} + \text{PL}_{0,\infty}$ protocol. As expected, we observe an oscillatory behavior of the TP as a function of Δ_2 . Moreover, $|\Delta\Phi|/2\pi$ is also plotted as a function of Δ_2 which shows a linear dependence as a function of Δ_2 . In the range that $\Delta\Phi$ oscillates, i.e., between $-\pi$ and π , \mathcal{P} attains its maximum at places where $\Delta\Phi \simeq 0$ and becomes zero at $|\Delta\Phi| = \pi$.

In Fig. 7(b), $\mathcal{P}_{\text{GL}}^{(4)}$ is plotted as a function of the linear coupling Δ_1 . In stark difference with gapped models, $\mathcal{P}_{\text{GL}}^{(4)}$ does not show any change of interference between the two peaks since $|\Delta\Phi| = \pi$ is constant as a function of Δ_1 . This

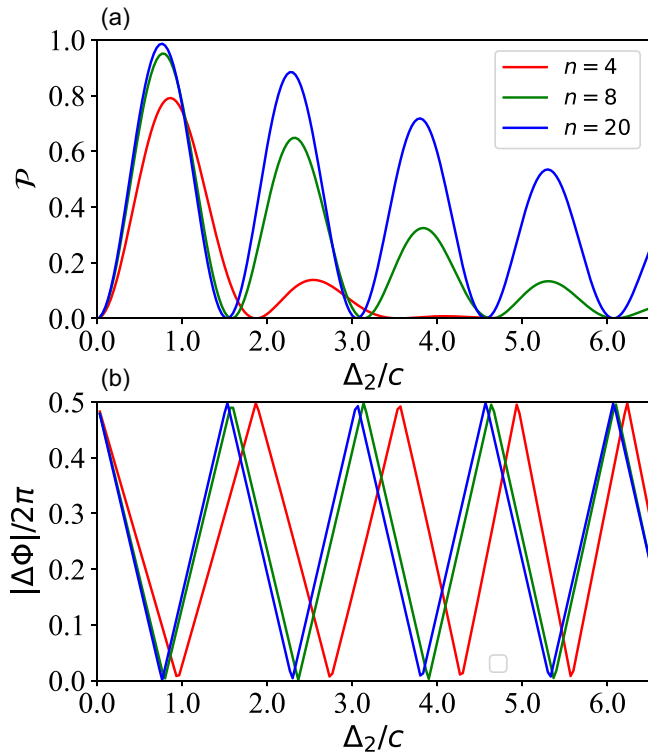


FIG. 8. (a) $\mathcal{P}_{\text{GP}}^{(n)}$ as a function of Δ_2/c for a PL_2 protocol with $n = 4, 8, 20$. (b) The corresponding $|\Delta\Phi|/2\pi$ as a function of Δ_2/c .

leads to the absence of oscillations for the \mathcal{P} as a function of Δ_1 .

The main reason for the linear dependence of $\Delta\Phi$ as a function of Δ_2 for gapped models could be understood as follows. For a PL_2 protocol, there is a region between $\lambda_{\pm, \text{MFP}}$, where $\chi \simeq 0$ and there is no transition. If one writes the evolved state based on eigenstates in this region, the only thing that happens in this region is the accumulation of phases for each instantaneous eigenstates during the evolution. Since, the dispersion of energies is almost flat in this region (see Fig. 2), the phase difference between the two states becomes $\Delta\Phi = \left[\int_{-\lambda_{-, \text{MFP}}}^{\lambda_{+, \text{MFP}}} \frac{(E_2 - E_1)}{c} d\lambda \right]_{\text{mod } 2\pi} = [4\lambda_{+, \text{MFP}} \Delta_2/c]_{\text{mod } 2\pi}$. When $n \gg 1$, then $\lambda_{+, \text{MFP}} \rightarrow 1$. Therefore, $\Delta\Phi = [4\Delta_2/c]_{\text{mod } 2\pi}$, is expected. For smaller values of n the region with $\chi \simeq 0$ shrinks, consequently phase and probability oscillations show a larger period. In Fig. 8(a), we plot $\mathcal{P}^{(n)}$ for different values of n

as a function of Δ_2/c . In Fig. 8(b), the same is depicted for $|\Delta\Phi|/2\pi$. The period of oscillations approaches to $\pi/2$ for larger n , where it is slightly larger for $n = 4$ due to the shrunk $\chi \simeq 0$ region in comparison to $n = 20$, which is in agreement with our analysis.

The absence of the change of interference in gapless models could be understood based on the fact that the levels cross and the sign of energy levels changes symmetrically by a passage through the touching point. Thus, dynamical phase accumulations cancel out in the region of small χ , and the interference will not depend on the linear coupling.

VI. CONCLUSION

In conclusion, by looking at FIS (χ), we investigated the nonadiabatic transition for gapless TLSs with a single touching point in their spectrum as a function of some parameter λ . We showed that as long as there exists certain types of quadratic terms in the Hamiltonian (as a function of λ), the low-energy form could not be approximated with a linear one even in the arbitrary vicinity of the touching point. That is, $\chi(\lambda) \neq 0$ as $\lambda \rightarrow 0$. This results in \mathcal{P} (the TP) becoming less than one by passing through the touching point.

We further showed that in the absence of quadratic terms, the low-energy Hamiltonian could be well approximated with a linear one in the sufficient vicinity of the touching point (even with the presence of terms with exponents larger than two). Here, $\chi(\lambda) \rightarrow 0$ as $\lambda \rightarrow 0$. Noticeably, terms with larger exponents than two do affect χ away from the touching point through the extant of a double peak in the dispersion of χ as a function of λ (please see the main text for the definition of the exact form of the Hamiltonians we have considered). In comparison with gapped models, the TP does not show any oscillation as a function of the linear coupling, which is the signature of the absence of the change of interference between two peaks. The reason for the lack of oscillations in this case is the change of the sign of the energies associated to instantaneous eigenstates by passing through the touching point. Consequently, phase accumulation does not occur, which in turn leads to the absence of interference between two peaks as a function of the linear coupling.

ACKNOWLEDGMENT

We thank Abolhassan Vaezi for helpful discussions and carefully reading our paper.

[1] H. Nakamura, *Nonadiabatic Transition* (World Scientific, Singapore, 2002).
 [2] S. Shevchenko, S. Ashhab, and F. Nori, Landau-Zener-tückelberg interferometry, *Phys. Rep.* **492**, 1 (2010).
 [3] M. Heyl, Dynamical quantum phase transitions: A review, *Rep. Prog. Phys.* **81**, 054001 (2018).
 [4] S. E. deGraaf, L. Faoro, L. B. Ioffe, S. Mahashabde, J. J. Burnett, T. Lindström, S. E. Kubatkin, A. V. Danilov, and A. Ya. Tzalenchuk, Two-level systems in superconducting quantum devices due to trapped quasiparticles, *Sci. Adv.* **6**, eabc5055 (2020).

[5] S. Ashhab, J. R. Johansson, and F. Nori, Decoherence in a scalable adiabatic quantum computer, *Phys. Rev. A* **74**, 052330 (2006).
 [6] I. M. Georgescu, S. Ashhab, and F. Nori, Quantum simulation, *Rev. Mod. Phys.* **86**, 153 (2014).
 [7] A. M. Zagoskin, S. Ashhab, J. R. Johansson, and F. Nori, Quantum Two-Level Systems in Josephson Junctions as Naturally Formed Qubits, *Phys. Rev. Lett.* **97**, 077001 (2006).
 [8] C. Müller, J. H. Cole, and J. Lisenfeld, Towards understanding two-level-systems in amorphous solids: Insights from quantum circuits, *Rep. Prog. Phys.* **82**, 124501 (2019).

- [9] L. D. Landau, On the Theory of Transfer of Energy at Collisions II, *Phys. Z. Sowjetunion* **2**, 46 (1932).
- [10] E. Stückelberg, Theory of inelastic collisions between atoms, *Helv. Phys. Acta* **5**, 369 (1932).
- [11] C. Zener and R. H. Fowler, Non-adiabatic crossing of energy levels, *Proc. R. Soc. London A* **137**, 696 (1932).
- [12] S. Gustavsson, J. Bylander, and W. D. Oliver, Time-reversal Symmetry and Universal Conductance Fluctuations in a Driven Two-Level System, *Phys. Rev. Lett.* **110**, 016603 (2013).
- [13] S. Ashhab, Landau-Zener transitions in a two-level system coupled to a finite-temperature harmonic oscillator, *Phys. Rev. A* **90**, 062120 (2014).
- [14] L. Arceci, S. Barbarino, R. Fazio, and G. E. Santoro, Dissipative Landau-Zener problem and thermally assisted quantum annealing, *Phys. Rev. B* **96**, 054301 (2017).
- [15] R. K. Malla and M. E. Raikh, Landau-Zener transition in a two-level system coupled to a single highly excited oscillator, *Phys. Rev. B* **97**, 035428 (2018).
- [16] R. K. Malla, V. Y. Chernyak, and N. A. Sinitsyn, Nonadiabatic transitions in Landau-Zener grids: Integrability and semiclassical theory, *Phys. Rev. B* **103**, 144301 (2021).
- [17] J. Lehto and K.-A. Suominen, Superparabolic level-glancing models for two-state quantum systems, *Phys. Rev. A* **86**, 033415 (2012).
- [18] N. V. Vitanov and K.-A. Suominen, Nonlinear level-crossing models, *Phys. Rev. A* **59**, 4580 (1999).
- [19] J. Lehto, Zhu-Nakamura theory and the superparabolic level-glancing models, *Phys. Rev. A* **88**, 043404 (2013).
- [20] K.-A. Suominen, Parabolic level crossing models, *Opt. Commun.* **93**, 126 (1992).
- [21] J.-N. Fuchs, L.-K. Lim, and G. Montambaux, Interband tunneling near the merging transition of Dirac cones, *Phys. Rev. A* **86**, 063613 (2012).
- [22] R. K. Malla and M. E. Raikh, High Landau levels of two-dimensional electrons near the topological transition caused by interplay of spin-orbit and zeeman energy shifts, *Phys. Rev. B* **99**, 205426 (2019).
- [23] K. S. Novoselov, A. K. Geim, S. V. Morozov, D. Jiang, M. I. Katsnelson, I. V. Grigorieva, S. V. Dubonos, and A. A. Firsov, Two-dimensional gas of massless Dirac fermions in graphene, *Nature (London)* **438**, 197 (2005).
- [24] A. K. Geim and K. S. Novoselov, The rise of graphene, *Nat. Mater.* **6**, 183 (2007).
- [25] A. H. Castro Neto, F. Guinea, N. M. R. Peres, K. S. Novoselov, and A. K. Geim, The electronic properties of graphene, *Rev. Mod. Phys.* **81**, 109 (2009).
- [26] M. Goerbig and G. Montambaux, Dirac fermions in condensed matter and beyond, in *Dirac Matter*, edited by B. Duplantier, V. Rivasseau, and J.-N. Fuchs (Springer International Publishing, Cham, 2017), pp. 25–53.
- [27] A. Y. Kitaev, Unpaired Majorana fermions in quantum wires, *Phys. Usp.* **44**, 131 (2001).
- [28] G. E. Volovik, Fermion zero modes on vortices in chiral superconductors, *J. Exp. Theor. Phys. Lett.* **70**, 609 (1999).
- [29] B. Bernevig and T. Hughes, *Topological Insulators and Topological Superconductors* (Princeton University Press, Princeton, NJ, 2013).
- [30] V. Pardo and W. E. Pickett, Half-Metallic Semi-Dirac-Point Generated by Quantum Confinement in TiO_2/VO_2 Nanostructures, *Phys. Rev. Lett.* **102**, 166803 (2009).
- [31] H. Huang, Z. Liu, H. Zhang, W. Duan, and D. Vanderbilt, Emergence of a Chern-insulating state from a semi-Dirac dispersion, *Phys. Rev. B* **92**, 161115(R) (2015).
- [32] S. Banerjee and W. E. Pickett, Phenomenology of a semi-Dirac semi-Weyl semimetal, *Phys. Rev. B* **86**, 075124 (2012).
- [33] M. Milićević, G. Montambaux, T. Ozawa, O. Jamadi, B. Real, I. Sagnes, A. Lemaître, L. Le Gratiet, A. Harouri, J. Bloch, and A. Amo, Type-III and Tilted Dirac Cones Emerging from Flat Bands in Photonic Orbital Graphene, *Phys. Rev. X* **9**, 031010 (2019).
- [34] L. Tarruell, D. Greif, T. Uehlinger, G. Jotzu, and T. Esslinger, Creating, moving and merging Dirac points with a Fermi gas in a tunable honeycomb lattice, *Nature (London)* **483**, 302 (2012).
- [35] M. Polini, F. Guinea, M. Lewenstein, H. C. Manoharan, and V. Pellegrini, Artificial honeycomb lattices offer a tunable platform for studying massless Dirac quasiparticles, and their topological and correlated phases, *Nat. Nanotechnol.* **8**, 625 (2013).
- [36] T. Uehlinger, G. Jotzu, M. Messer, D. Greif, W. Hofstetter, U. Bissbort, and T. Esslinger, Artificial Graphene with Tunable Interactions, *Phys. Rev. Lett.* **111**, 185307 (2013).
- [37] E. Altman, K. R. Brown, G. Carleo, L. D. Carr, E. Demler, C. Chin, B. DeMarco, S. E. Economou, M. A. Eriksson, Kai-Mei C. Fu, M. Greiner, K. R. A. Hazzard, R. G. Hulet, A. J. Kollár, B. L. Lev, M. D. Lukin, R. Ma, X. Mi, S. Misra, C. Monroe *et al.*, Quantum simulators: Architectures and opportunities, *PRX Quantum* **2**, 017003 (2021).
- [38] G. Montambaux, F. Piéchon, J.-N. Fuchs, and M. O. Goerbig, A universal Hamiltonian for motion and merging of Dirac points in a two-dimensional crystal, *Eur. Phys. J. B* **72**, 509 (2009).
- [39] M. I. Katsnelson, *Graphene: Carbon in Two Dimensions* (Cambridge University Press, Cambridge, UK, 2012).
- [40] L.-K. Lim, J.-N. Fuchs, and G. Montambaux, Bloch-Zener Oscillations Across a Merging Transition of Dirac Points, *Phys. Rev. Lett.* **108**, 175303 (2012).
- [41] Y. Sun, D. Leykam, S. Nenni, D. Song, H. Chen, Y. D. Chong, and Z. Chen, Observation of valley Landau-Zener-Bloch Oscillations and Pseudospin Imbalance in Photonic Graphene, *Phys. Rev. Lett.* **121**, 033904 (2018).
- [42] L.-K. Lim, J.-N. Fuchs, and G. Montambaux, Mass and Chirality Inversion of a Dirac Cone Pair in Stückelberg Interferometry, *Phys. Rev. Lett.* **112**, 155302 (2014).
- [43] J. Xu, Probing the energy spectrum in the vicinity of Dirac points with Landau-Zener transition, *Commun. Theor. Phys.* **62**, 343 (2014).
- [44] T. Uehlinger, D. Greif, G. Jotzu, L. Tarruell, T. Esslinger, L. Wang, and M. Troyer, Double transfer through Dirac points in a tunable honeycomb optical lattice, *Eur. Phys. J.: Spec. Top.* **217**, 121 (2013).
- [45] W.-L. You, Y.-W. Li, and S.-J. Gu, Fidelity, dynamic structure factor, and susceptibility in critical phenomena, *Phys. Rev. E* **76**, 022101 (2007).
- [46] M. Tomka, A. Polkovnikov, and V. Gritsev, Geometric Phase Contribution to Quantum Nonequilibrium Many-Body Dynamics, *Phys. Rev. Lett.* **108**, 080404 (2012).

- [47] L. Wang, Y.-H. Liu, J. Imriška, P. N. Ma, and M. Troyer, Fidelity Susceptibility Made Simple: A Unified Quantum Monte Carlo Approach, *Phys. Rev. X* **5**, 031007 (2015).
- [48] S.-J. Gu, Fidelity susceptibility and quantum adiabatic condition in thermodynamic limits, *Phys. Rev. E* **79**, 061125 (2009).
- [49] D. N. Esfahani, L. Covaci, and F. M. Peeters, Nonlinear response to electric field in extended Hubbard models, *Phys. Rev. B* **90**, 205121 (2014).
- [50] A. Dykhne, Quantum transitions in the adiabatic approximation, *Sov. Phys. JETP* **11**, 411 (1960).
- [51] J. P. Davis and P. Pechukas, Nonadiabatic transitions induced by a time-dependent Hamiltonian in the semiclassical/adiabatic limit: The two-state case, *J. Chem. Phys.* **64**, 3129 (1976).
- [52] T. Oka, R. Arita, and H. Aoki, Breakdown of a Mott Insulator: A Nonadiabatic Tunneling Mechanism, *Phys. Rev. Lett.* **91**, 066406 (2003).